

## Rupture of an extended object: A many-body Kramers calculation

Anirban Sain,<sup>1,\*</sup> Cristiano L. Dias,<sup>2,†</sup> and Martin Grant<sup>2</sup>

<sup>1</sup>*Physics Department, Indian Institute of Technology-Bombay, Powai 400076, India*

<sup>2</sup>*Physics Department, McGill University, Rutherford Building, 3600 rue University, Montreal, QC, Canada H3A 2T8*

(Received 11 April 2006; published 16 October 2006)

We show how an extended object's strain field is redistributed when the material ruptures under by thermal activation. Through analytical calculations and molecular dynamics simulations, we show that in a polymer chain the distribution is exponentially localized around the point of rupture. The length scale of localization is determined by the strain and microscopic parameters of the interaction potential. We also derive an analytic expression for the rate of bond rupture by consistently treating the collective modes of the chain and the effect of dissipation on those modes. Our theoretical estimates are of the same order of magnitude as those obtained by simulations, as compared to earlier theories which had overestimated the rate of rupture by approximately two orders of magnitude. It is also noteworthy that the correction comes about through the effective attempt frequency rather than the effective barrier height.

DOI: [10.1103/PhysRevE.74.046111](https://doi.org/10.1103/PhysRevE.74.046111)

PACS number(s): 05.40.-a, 82.39.-k, 82.20.Uv, 02.50.Ey

### I. INTRODUCTION

In this paper we study the rupture of a bond in the middle of a stretched linear polymer chain using a multidimensional version of Kramers rate theory [1]. This formalism is significantly different from the commonly used multidimensional transition state theory and gives rather accurate predictions for the truly nonequilibrium breakage phenomena. Mechanochemistry, including experimental realization of such polymers, can be found in Ref. [2]. We consider the case where the polymer is modeled as a chain of monomers connected to its nearest neighbors by a Lennard-Jones interaction. The coupled dynamics of these molecules is essentially a many-body problem since strong correlation effects arise from the collective modes of the polymer chain. Despite previous work by computer simulation [3–5] and theory [6], a clear understanding of this problem has not yet emerged. In previous theoretical work, the many-body problem has been argued, variously, to be equivalent to an effective one-body problem [3], or that the effect of friction on the collective modes can be treated phenomenologically [6,7]. The theoretical estimates obtained for the rate of rupture from these methods can be two orders of magnitude higher than those observed in simulations, suggesting that further theoretical investigation is warranted. In this paper, we explore the kinetics of the collective breakage mode that causes rupture, and in particular we illustrate the pathway of excitations leading to the rupture of a single bond. Using both an analytic calculation and molecular dynamics simulations, we establish the spatiotemporal behavior of the chain of masses during its rupture. In particular, our analytic calculation of the breakage rate is within a factor of 4 of our estimate from numerical simulation.

We model a stretched polymer as a one-dimensional chain of  $N$  beads constrained between fixed walls. The constant length of the chain is  $N(a+s)$ , where  $a$  is the equilibrium

bond length and  $s$  is the applied strain. The interaction between first-neighbor beads is described by a Lennard-Jones potential  $V(r) = \epsilon[(a/r)^{12} - 2(a/r)^6]$ , where  $\epsilon$  is the binding energy. The dynamics of this chain is obtained by solving a Langevin equation for the position  $u_i$  of each bead:

$$m \frac{d^2 u_i}{dt^2} = F(u_i - u_{i-1}) - F(u_{i+1} - u_i) - m\gamma \frac{du_i}{dt} + f_i(t), \quad (1)$$

where  $F(x)$  is the force computed from the potential,  $m$  is the mass of the bead, and  $\gamma$  is the friction coefficient. The fixed wall boundary condition implies  $u_0 = u_{N+1} = 0$ . The random, Gaussian force  $f_i(t)$  is related to  $\gamma$  by a fluctuation-dissipation theorem.

Our analytic calculation is based on a phase space formalism due to Langer [1,8,9]. This many-body formalism seeks out the unique escape direction across a saddle point in the  $2N$ -dimensional phase space. This saddle point has  $2N-1$  stable directions and a single unstable direction. The growth rate of the unstable collective mode along this direction determines the escape rate. Technically, the determination of the growth rate amounts to extracting the unique positive eigenvalue  $\lambda_+$  of a  $2N \times 2N$ -dimensional matrix in phase space. This dynamical matrix results from a quadratic approximation of the interaction potential and it also accounts for the friction term [of Eq. (1)] through a velocity dependent potential  $\frac{\gamma}{2} \dot{u}_i^2$ .

In principle, the snapping of the polymer can occur via many pathways, and our treatment restricts the possible paths considered. The breakage rate which we compute here is that for a single bond. The simultaneous rupture of two or more bonds can be straightforwardly estimated as exponentially rare, compared to a single bond rupture [10].

The quadratic approximation of the Hamiltonian restricts our treatment of configuration space to that where all the  $(N-1)$  bonds are in their respective quadratic wells and the breaking bond is near the barrier. However, our simulations show that at high temperatures, fluctuations of individual bond lengths near the breaking bond are larger than what can be described within a harmonic approximation. This weak-

\*Electronic address: [asain@phy.iitb.ac.in](mailto:asain@phy.iitb.ac.in)

†Electronic address: [diasc@physics.mcgill.ca](mailto:diasc@physics.mcgill.ca)

ness, also shared by the classical Kramers theory [11] for a single particle, might explain some of the mismatch seen when we compare our theoretical estimates with simulations.

The paper is organized as follows. Section II contains the analytical calculation of chain rupture, namely the rupture profile and the rate. In Sec. III we present results from molecular dynamics simulations, and compare the numerically obtained profile with our theoretical prediction. The theoretical rate of rupture is compared to simulation in Sec. IV.

## II. THEORY

To compute the probability that any of the bonds in the polymer snaps, we use multidimensional Kramers theory [1] for the escape of a particle from a metastable state. This theory is different from the multidimensional transition state theory in the same way as Kramers single particle escape rate theory differs from transition state theory. In particular, Kramers theory captures the nonequilibrium effects of the bath friction in a consistent way and can naturally include the recrossing events in computing the net escape rate. Transition state theory cannot do this, and thus typically overestimates the escape rate. Kramers formalism computes the net, outward probability flux across the barrier using the true nonequilibrium phase-space probability density.

For the model polymer of interest here, the metastable state corresponds to the stretched, static equilibrium configuration where all the bonds are intact. The stable state corresponds to the configuration where one of the bonds is broken and the snapped chain is relaxed. The transition from the metastable to the stable state occurs via an unstable transition state, which represents an overstretched bond near its breaking threshold. The main result of Kramers theory for a single particle is the escape rate  $\Gamma$ , given by

$$\Gamma = \frac{\lambda_+}{2\pi} R e^{-E_b/k_B T}, \quad (2)$$

where  $E_b$  is the barrier height and  $R = \omega_s/\omega_u$  is the ratio of frequencies associated with the curvature of the trapping potential  $V(r)$  at the respective metastable (subscript  $s$ ) and unstable (subscript  $u$ ) equilibrium points via  $\omega_{s,u}^2 \equiv \frac{1}{m} |V''_{s,u}|$ . The factor

$$\lambda_+ = \frac{1}{2} (\sqrt{\gamma^2 + 4\omega_u^2} - \gamma) \quad (3)$$

can be obtained by solving for the unstable eigenmode  $x(t) = \exp(\lambda_+ t)$  of the unforced equation

$$m\ddot{x} = -\gamma m\dot{x} + \omega_u^2 x, \quad (4)$$

where a quadratic approximation to the potential near the barrier,  $V(x) = E_b - \frac{1}{2}\omega_u^2 x^2$ , has been used. Note that the absence of noise in the above equation does not mean the effect of noise is neglected in deriving the Kramers result. In fact, it can be rigorously shown [1,12] that the solution of the equivalent Fokker-Plank equation amounts to solving for  $\lambda_+$  from the unforced equation of motion.

For a many-body problem [1], the form of the rate expression [Eq. (2)] remains the same, but to obtain  $\lambda_+$  one must

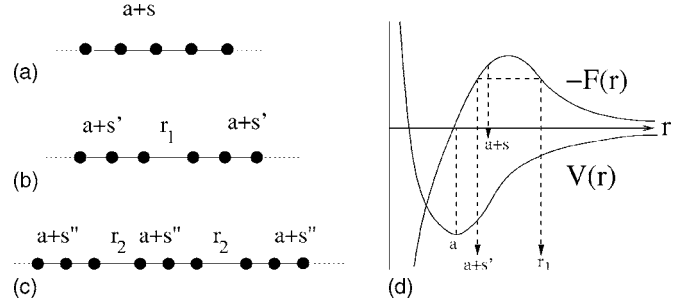


FIG. 1. (a) Stable and (b), (c) unstable equilibrium configurations for one and two breakages, respectively. In (d) negative of the elastic forces  $-F(r) = V'(r)$  for the respective bond lengths are denoted.

solve the unforced, coupled, linear set of equations for the whole chain. The computation of the prefactor  $R$  in the rate expression remains the same as in multidimensional transition state theory. The first instance of Langer's formalism applied to a polymeric system was reported in Ref. [8]. For the particular polymer problem which we discuss here, the solution for  $\lambda_+$  is outlined below.

Using a harmonic approximation around the equilibrium configuration, the equations of motion for the monomers, except the ones neighboring the broken bond, are given by

$$m\ddot{u}_j = K(u_{j+1} - 2u_j + u_{j-1}) - \gamma\dot{u}_j; \quad j \neq n, n+1, \quad (5)$$

where  $u_j$  now stands for the displacement from the equilibrium position [unlike in Eq. (1)]. For the  $n$  and  $(n+1)$ -th monomers, which are driven apart during rupture, the equations of motion in the harmonic approximation are

$$m\ddot{u}_n = K'(u_{n+1} - u_n) - K(u_n - u_{n-1}) - \gamma\dot{u}_n, \quad (6)$$

$$m\ddot{u}_{n+1} = K(u_{n+2} - u_{n+1}) - K'(u_{n+1} - u_n) - \gamma\dot{u}_{n+1}, \quad (7)$$

where  $K$  and  $K'$  are the effective spring constants of the locally harmonic bonds. In order to relate these quantities to the actual interaction potential, we analyze the static equilibrium configuration of the system.

The system has three static equilibrium points where force balance can be achieved. One of these corresponds to the trivial equilibrium configuration after rupture when the applied strain  $s$  is released and all except the broken bond settles down to their equilibrium length  $a$ . Among the other two points, one is stable and the other is unstable. The stable equilibrium point corresponds to a uniformly stretched polymer with each bond length equal to  $a+s$  [13]. In order to describe the motion around this point, we set  $K' = K = V''(r = a+s)$  in Eqs. (5)–(7). Here  $V''(r)$  is the second derivative of the interaction potential.

The origin of the unstable point can be understood from Fig. 1 which illustrates a typical interatomic potential  $V(r)$ , and the corresponding elastic force  $F(r) = -V'(r)$ . At static equilibrium all the bonds experience an equal stretching force. From Fig. 1, we note that same force can be obtained for, say, two different bond lengths  $\ell = a+s'$  and  $r_1$ , where  $s'$  is the residual strain in the non-breaking bonds. But at  $\ell = a+s'$  the bond is stable while at  $\ell = r_1$  it is unstable. So

the chain can have a static configuration where one bond has a length  $r_1$  and the other bonds have length  $\ell = a + s'$ , with the constraint  $(N-1)(a+s') + r_1 = N(a+s)$ . To describe the motion around this unstable point, we set the curvatures in Eqs. (5)–(7) to  $K = V''(a+s')$  and  $K' = V''(r_1)$ . This unstable equilibrium corresponds to the saddle point which leads to rupture. Finally, we note that, in the context of transition-state theory, this unstable point corresponds to the transition state. Thus the energy barrier is given by the excess energy of this state:

$$E_b = [V(r_1) + (N-1)V(a+s')] - NV(a+s). \quad (8)$$

Similarly, we can find other unstable static configurations where two bonds are unstable with  $\ell = r_2$ , and the rest are stable with  $\ell = a + s''$ ; see Fig. 1(c).

Now we turn to the problem of finding the solution of Eqs. (5)–(7) around the static equilibrium configurations (a) and (b) in Fig. 1) discussed above. When the chain is at stable equilibrium (a), all the bonds are in their metastable wells and thus  $K' = K > 0$ . Then the solutions of Eq. (5) for  $j \leq n$  is  $u_j = \exp(i\omega t) \sin kj$ , while for  $j \geq n+1$ , we have  $u_j = A \exp(i\omega t) \sin kj$ . These solutions yield the dispersion relation

$$\omega_j = i \frac{\gamma}{2m} \left( 1 + \sqrt{1 - \frac{8Km}{\gamma^2} (1 - \cos kj)} \right), \quad (9)$$

where the allowed modes are given by  $k_j = \frac{\pi j}{N+1}$ , where  $j \in [1, N]$ , consistent with the boundary conditions. Complex frequencies above imply that modes die out at a rate determined by the friction coefficient  $\gamma$ . Substituting these solutions into either Eq. (6) or Eq. (7) gives the relative amplitude  $A$ . One can show that  $A = 1$  when  $K = K'$ .

At the unstable equilibrium configuration, when  $K' < 0$ , there are  $(N-1)$  stable modes and one unstable mode. The unstable mode leading to breakage can be described by  $u_j = -\exp(\lambda_+ t) \sinh kj$  for  $j \leq n$  and  $u_j = A \exp(\lambda_+ t) \sinh k(N+1-j)$  for  $j \geq n+1$ . Note that this mode is consistent with the rupture of a bond as it produces a discontinuity in displacement about that bond. These solutions satisfy Eq. (5), with the respective boundary conditions, and they give the eigenvalue of the unstable mode:

$$\lambda_+ = \frac{\gamma}{2m} \left( \sqrt{1 + \frac{8mK}{\gamma^2} (\cosh k - 1)} - 1 \right). \quad (10)$$

The unknown mode factor  $k$  and the amplitude  $A$  have to be determined from the boundary equations, Eqs. (6) and (7). These equations yield

$$\begin{aligned} A(c_1 - c_2) \sinh k(N-n-1) + 2 \sinh kn \\ = [c_1 + c_2] \sinh k(n-1), \end{aligned} \quad (11)$$

$$\begin{aligned} A(c_1 + c_2) \sinh k(N-n-1) - 2 \sinh k(N-n) \\ = [c_1 - c_2] \sinh k(n-1), \end{aligned} \quad (12)$$

where  $c_1 = 1/(2 \cosh k - 1)$  and  $c_2 = 1/(2 \cosh k + 2K'/K - 1)$ . These can be numerically solved to obtain  $A$  and  $k$  for arbitrary  $n < N$ .

If the bond which breaks lies exactly at the middle of the chain, the above equations simplify and become analytically tractable. Then it is easy to show that the relative amplitude  $A = 1$ , and for  $k$ , we obtain a transcendental equation

$$2 \cosh k + 2K'/K - 1 = \frac{\sinh k(n-1)}{\sinh kn}, \quad (13)$$

by equating  $c_2$  obtained from any of these equations with its definition. This transcendental equation must be solved for  $k$ . Henceforth we will focus on this case which can be straightforwardly compared to simulations with periodic boundary condition. If  $n$  is large ( $n = N/2 \geq 50$  in our simulation), and  $k$  is of order 1, then the right hand side can be approximated by  $e^{-k}$  and we obtain  $k \approx \ln(1 - 2K'/K)$ . Once  $k$  is found, the growth rate  $\lambda_+$  of the unstable mode can be calculated in Eq. (10). It is straightforward to consider the case for the bond breaking at another position in the polymer. By solving the transcendental equation numerically, we find that the breakage rate reduces slowly as the rupturing bond ( $n'$ ) shifts towards the fixed walls. Note that  $k$  is independent of the friction  $\gamma$  and depends only on the properties of the interaction potential. The breakage profile remains unchanged if  $\gamma$  is tuned, but its growth in time, which depends on  $\lambda_+$ , is controlled by  $\gamma$ . In the large friction limit, expanding the formula in Eq. (10) in powers of  $\gamma^{-1}$  we obtain  $\lambda_+ = 4K(\cosh k - 1)/\gamma$ , i.e.,  $\lambda_+ \sim \gamma^{-1}$  as in standard Kramers theory. In order to compute the attempt frequency for rupture, defined as  $\nu \equiv \lambda_+ R/2\pi$ , one still needs to compute  $R$ . In the multibody framework [1],  $R$  is given by

$$R \equiv |\det \mathbf{E}^{(s)} / \det \mathbf{E}^{(u)}|^{1/2}, \quad (14)$$

where  $\mathbf{E}^{(s)}$  and  $\mathbf{E}^{(u)}$  are the Hessians at the stable and unstable fixed points, respectively. They share a common tridiagonal structure with their nonzero off-diagonal elements equal to  $-1$  and their  $N$  diagonal elements are  $K_s[2, 2, \dots, 2, 2, \dots, 2]$  for  $\mathbf{E}^{(s)}$ , and  $K[2, 2, \dots, 2, (1 + \frac{K'}{K}), (1 + \frac{K'}{K}), 2, 2, \dots, 2]$  for  $\mathbf{E}^{(u)}$ , where the  $(N/2)$ -th and  $(N/2+1)$ -th diagonal elements are  $(1 + \frac{K'}{K})$ . Note once again that  $K_s \equiv V''(a+s)$  and  $K \equiv V''(a+s')$  are both positive, while  $K' \equiv V''(r_1)$  is negative. We evaluate  $\det \mathbf{E}^{(u)}$  numerically, while one can show that  $\det \mathbf{E}^{(s)} = (N+1)(K_s)^N$ .

### III. SIMULATION

We now present the results of our numerical simulations of the model in order to check our theoretical predictions. We use the Lennard-Jones potential and show that the profile of bond lengths around the broken bond agrees with the one computed analytically. First we define the order parameter for rupture as being the length of the largest bond of the chain. The larger this parameter is, the closer to rupture is the chain. The bond length profile is then computed for different values of this parameter, that is, at different instants along rupture. A comparison with the analytical calculation is then provided.

For simplicity we use reduced units. Energy is given in units of  $\epsilon$ , distance is given in terms of  $a$ , and time is given in units of the smallest phonon oscillation period  $\tau_0$



$=2\pi/[12\sqrt{(2\epsilon/ma^2)}$  of the intact chain, obtained from the dispersion relation given before. Mass is written in terms of  $m$  and the friction coefficient is tuned to  $\gamma=0.25(2\pi/\tau_0)$ . In this paper, simulations are performed with chains containing up to  $N=200$  beads.

We start the simulation with a uniformly stretched chain having all the bonds stretched by the same amount  $S$ . The velocity of each atom is chosen randomly following a Boltzmann distribution. The dynamics are simulated by numerically integrating the equations of motion [Eq. (1)] with the velocity-Verlet algorithm [14]. Due to the stochastic nature of rupture, 800 chains (each containing 200 atoms) were used for statistics. Although the analytical calculations were performed with chains having fixed walls, periodic boundary conditions are used in the simulation. The choice of periodic boundary condition in the simulation facilitates averaging over different chains since, irrespective of the position of rupture, the breaking bond can always be considered at the center of the chain.

In Fig. 2(a) we present the mean time  $\tau$  required for the length of the largest bond to reach different values  $d$ . These data were computed for a temperature of 0.018, in units of  $\epsilon$ , and an applied strain of 0.0325 (in units of  $a$ ). Details of the calculation scheme that leads to this figure can be found in Ref. [3]. Two distinct regimes are apparent. The first regime occurs when the length  $d$  of the largest bond is smaller than  $\sim 1.5$ , in units of  $a$ . In this case, the time required to produce an increase of  $d$  is appreciable. The underlying physics of this regime is the competition between thermal fluctuations, which are responsible for increasing the length of the largest bond, and the elastic restoring force on this bond. The second regime occurs when the length of the largest bond is greater than  $\sim 1.5$ . Here,  $\tau$  has reached a plateau: almost no time is required to increase the length of the largest bond. This occurs as the unstable point in the potential energy landscape is crossed, when the elastic force changes sign and becomes a breaking force for the largest bond. In that case, the bond cannot restore its equilibrium length and we can conclude that irreversible rupture has occurred. So, from Fig. 2(a) we can determine the value of  $d$  for which rupture occurs:  $d_c \sim 1.5$ . In the sense of a first-order phase transition, the length of the largest bond  $d$  can be interpreted as the order parameter determining how close a chain is to rupture.

Now, we study the profile of bond lengths as the chain approaches rupture. In particular, we compute the profile for the four values of  $d$  shown by arrows in Fig. 2(a). For each of the 800 chains, the profile of bond length is computed at the instant their largest bond length reaches the given values of  $d$ . We make use of periodic boundary condition to superpose the breakage points of the different chains and thereby compute an average. The mean profile obtained by this operation is shown in panels (b)–(e). Note that, past the breaking point, the length of the breaking bond becomes large while the neighboring bonds contract towards their unstretched equilibrium length  $a$ , so that the length of the whole chain is held fixed. To show the bond length profile in proper scale, in panels (b)–(e) we omit the value of the diverging bond length but indicate its position by an arrow. The solid line indicates the length  $a+s'$ , the bond length plus the residual strain, see Fig. 1.

Before discussing panels (b)–(e) of Fig. 2, we note that at any given time in the simulation the displacement field  $u(x,t)$  of the particles is a superposition of all the  $N$  modes. Only when one of the bonds tends towards breakage does an unstable mode develop. Since it is unstable, its growth is unidirectional (i.e., its amplitude retains its sign and grows in magnitude). In contrast, the amplitude of the other  $(N-1)$  stable modes being small fluctuates about zero due to friction and noise. Hence averaging over many chains helps to nullify the effect of the stable modes and picks out the contribution of the unstable mode.

In panel (b), where  $d=1.37$ , a few bonds close to the one that ruptures are compressed compared to the length  $a+s'$  that corresponds to the unstable static equilibrium. Among the different values of  $d$  shown in Fig. 2(a),  $d=1.37$  corresponds to the lowest value presenting such a localized compression. In the framework of normal modes, the unstable mode, leading to a localized strain profile, sets in at this point. The simulation shows that as the length of the largest bond increases further, the amplitude of the localized compression, corresponding to the amplitude of the unstable mode, becomes more pronounced, as illustrated in panels (c) and (d). In panel (e), the normal mode analysis cannot be applied since the chain has broken. However, we can still see a local compression profile which tends to broaden as  $d$  increases, since all nonruptured bonds tend to relax to their equilibrium length  $a$ . Thus this qualitative description of the pathway of rupture is consistent with the kinetics of the unstable mode.

Now we provide a quantitative comparison of our simulations to our theoretical predictions; see Fig. 3. According to theory, close to the rupture, the unstable mode dominates and thus the displacement field  $u_j(t)$  is proportional to

$$e^{\lambda t} \left[ -\theta\left(\frac{N}{2} - j\right) \sinh kj + \theta\left(j - \frac{N}{2}\right) \sinh k(N+1-j) \right], \quad (15)$$

where  $\theta(x)$  is the Heaviside step function. From this, the bond length profile is given by  $\ell_j=(a+s')+(u_{j+1}-u_j)=(a+s')+\partial_j u$ .

In Fig. 3 we fit  $\ell_j$ , as obtained from Eq. (15), to a bond length profile obtained from our simulation. This profile is chosen close to the instant of rupture, as in, e.g., Fig. 2(d). The wave number  $k$  was extracted from this fit and compared to the theoretical prediction. This yields  $k_s=0.267$  while the theoretical estimate [ $k \approx \ln(1-2K'/K)$ ] is  $k_t=0.32$ . Notice that it is difficult to isolate the unstable mode in the simulation. Even at the point of rupture where the unstable mode dominates, other modes are present. Also note that theory and simulation have different boundary conditions. Namely the theory uses fixed wall conditions while the simulation was performed on a ring geometry. Nevertheless, both boundary conditions share the crucial property that the fluctuations generate a fixed displacement ensemble instead of a fixed force ensemble. For large  $N$ , fixed displacement and fixed force ensembles are equivalent, but not so for short chains [15]. In the present context, since the rupture profile Eq. (15) is exponentially localized, as opposed to being

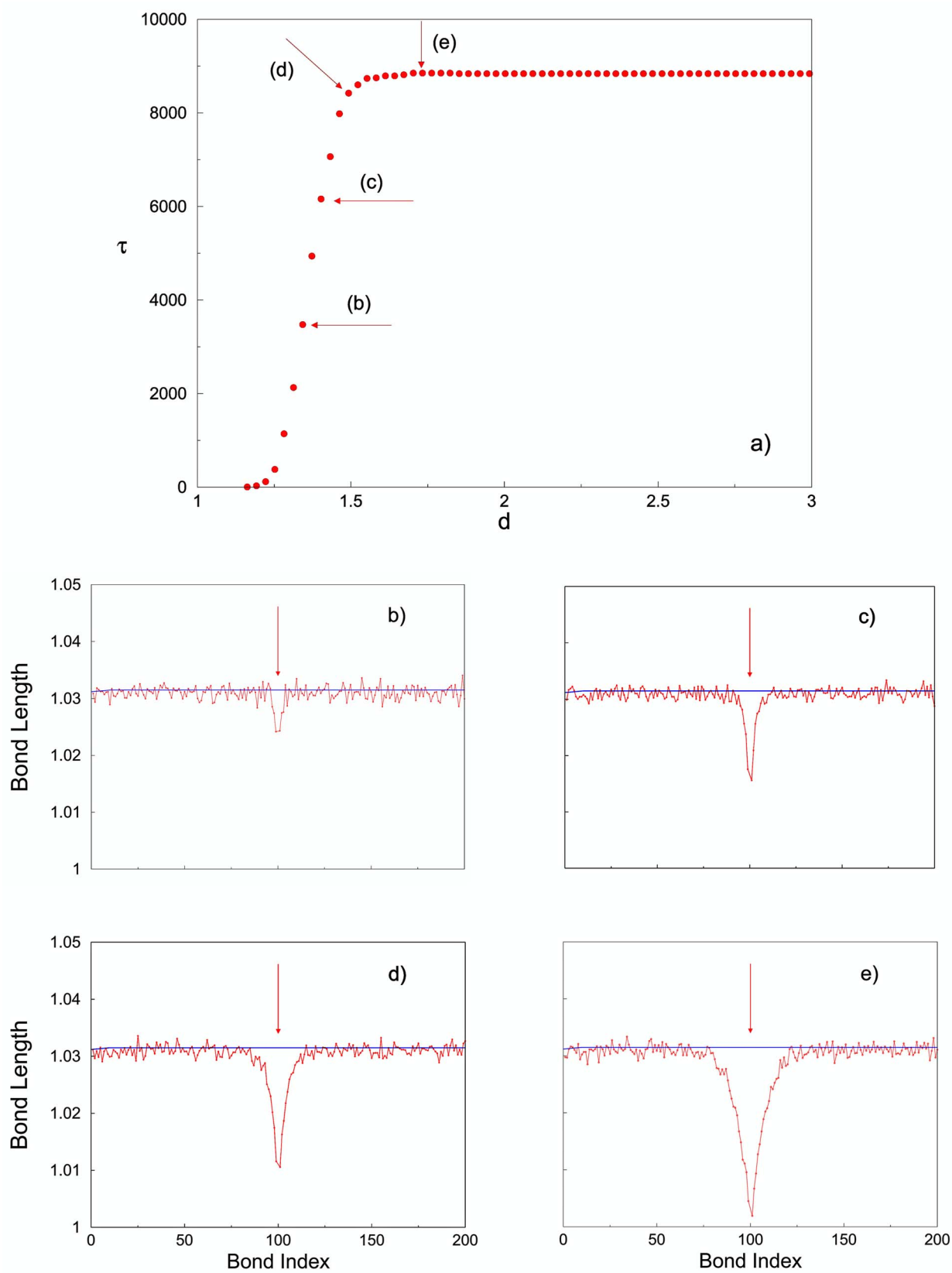


FIG. 2. (Color online) In (a) we show the mean time required to increase the length of the largest bond (for the first time) to a value  $d$ , in units of the bond length  $a$ . The profile of bond length is computed for each of the four states indicated by arrows. Panels (b)–(e) correspond to this profile. The line above the profile corresponds to  $a+s'$ , the bond length plus the residual strain. Dimensionless temperature is  $T=0.018$  and strain is  $s=0.0325$ .

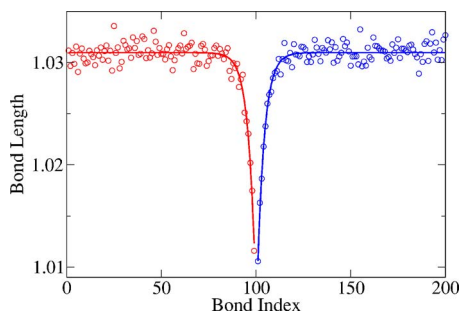


FIG. 3. (Color online) Bond lengths of all the 200 bonds (circle) of the chain during the breakage as seen in the simulation. The solid line is fit to the data with our theoretical prediction for  $\ell_n$ . The wave number  $k$  is extracted from the best fit. The bond which ruptures is omitted since its length is much larger than the rest.

spread out over the whole length of the system, the difference in boundary conditions is unlikely to be important. Our work also establishes that the previously unresolved large mismatch in breakage rate (200 times) between simulation and Kramers theory is not due to any subtle long range correlations [18], specific to low dimension.

#### IV. RATE OF RUPTURE

Finally, we compare the attempt frequency  $\nu$  and the energy barrier  $E_b$  obtained from simulation, to those calculated analytically. In the simulation, these quantities are extracted from the dependence of the logarithm of the breaking time on the inverse of temperature. The theoretical breakage rate is computed for one particular bond, whereas in the simulation any of the  $N$  bonds can break, so the theoretical attempt frequency is multiplied by  $N$  to give  $N\tau_0(\lambda_+R)/2\pi$ , where  $\lambda_+$  and  $R$  are given by Eqs. (10) and (14). The comparison is given in Table I.

The theoretical energy barriers are within 15% of those obtained numerically. This agreement was also observed in Refs. [3,16,17]. The theoretical attempt frequencies we obtain are within a factor of 4 of those obtained numerically. This is an improvement on previous theories which gave a frequency approximately two orders of magnitude larger than simulation results [3,6,19].

TABLE I. Comparison of the theoretical barrier and attempt frequency ( $E_b^t$  and  $\nu^t$ ) to the simulation ones ( $E_b^s$  and  $\nu^s$ ) for different values of strain. This comparison is performed for chains containing 100 atoms.

Strain ( $S$ )	0.0300	0.0325	0.0350	0.0375	0.0400
$\nu^t$	0.0263	0.0355	0.0462	0.058	0.0717
$\nu^s$	0.1044	0.1522	0.1412	0.1846	0.2739
$E_b^t$	0.187	0.163	0.141	0.122	0.105
$E_b^s$	0.169	0.147	0.119	0.103	0.092

We discuss a few possible reasons behind the mismatches between our theoretical estimate for attempt frequency ( $\nu^t$ ), rupture profile (wave number  $k_r$ ), and the simulation results ( $\nu^s, k_s$ ). (a) Kramers theory assumes that the trap is deep relative to  $kT$  such that the equilibration time is much smaller than the escape time, while in our simulations the trap depth is  $\sim 10kT$  to ensure that escape events are attainable within reasonable simulation time. (b) In order to obtain the breakage rate of a chain of  $N$  atoms, like other authors, we also assume that the breakage probability is  $N$  times the probability of breakage of one bond, since all bonds in the closed chain are equivalent. But kinematically, the instability of different bonds may not be independent events. (c) Few of the neighbors of the overstretched bond have their bond lengths in the nonquadratic region of the Lennard-Jones potential (see Figs. 2 and 3). That brings in nonlinear corrections and are beyond the reach of our present theoretical formalism.

In conclusion, we have found that the rupture of a single bond in a chain is a collective many-body effect [1,12]. Collective effects arise through the prefactor of the exponential in the rate formula, as dissipation drastically reduces the so-called attempt frequency, and through the exponential localization of the strain close to the rupturing bond. We expect that this latter feature is not special to our one-dimensional calculation, and that a similar exponential localization of the strain profile would follow in higher dimensions.

This work was supported by the Natural Sciences and Engineering Research Council of Canada, and *le Fonds Québécois de la recherche sur la nature et les technologies*.

- [1] J. Langer, *Ann. Phys. (N.Y.)* **54**, 258 (1969).
- [2] M. K. Beyer and H. C. Schaumann, *Chem. Rev. (Washington, D.C.)* **105**, 2921 (2005).
- [3] F. A. Oliveira and P. L. Taylor, *J. Chem. Phys.* **101**, 10118 (1994).
- [4] R. W. Welland, M. Shin, D. Allen, and J. B. Ketterson, *Phys. Rev. B* **46**, 503 (1992).
- [5] K. Bolton, S. Nordholm, and H. W. Schranz, *J. Phys. Chem.* **99**, 2477 (1995).
- [6] R. K. Puthur and K. L. Sebastian, *Phys. Rev. B* **66**, 024304 (2002).
- [7] K. Sebastian and R. Puthur, *Chem. Phys. Lett.* **304**, 399

(1999).

- [8] A. Sain and M. Wortis, *Phys. Rev. E* **70**, 031102 (2004).
- [9] L. Bongini, R. Livi, A. Politi, and A. Torcini, *Phys. Rev. E* **68**, 061111 (2003).
- [10] For a chain of 200 monomers, stretched by 3.25%, the energy barrier to break a single bond is  $8.72k_B T$  and that for two bonds simultaneously is  $18.11k_B T$  (see Fig. 1). Thus the ratio between the probabilities of double and single bond ruptures is  $\approx \exp(-9.4)$ , assuming attempt frequencies are of the same order.
- [11] H. Kramers, *Physica (Utrecht)* **7**, 284 (1940).
- [12] P. Hanggi, P. Talkner, and M. Borkovec, *Rev. Mod. Phys.* **62**,

- 251 (1990).
- [13] Frank H. Stillinger, Phys. Rev. E **52**, 4685 (1995).
- [14] M. P. Allen and D. J. Tildesley, *Computer Simulations of Liquids* (Clarendon, Oxford, 1990).
- [15] A. Dhar and D. Chaudhuri, Phys. Rev. Lett. **89**, 065502 (2002).
- [16] F. A. Oliveira, Phys. Rev. B **57**, 10576 (1998).
- [17] Cristiano L. Dias, M. Dube, F. A. Oliveira, and M. Grant, Phys. Rev. E **72**, 011918 (2005).
- [18] S. Lepri, P. Sandri, A. Politi Puthur, and K. L. Sebastian, Eur. Phys. J. B **47**, 549 (2005).
- [19] This mean-field type theory predicts that while the length of one bond is increasing towards rupture, the strain on the other bonds is equally distributed such as to satisfy the constraint of constant length for the chain. The energetics of the chain can then be obtained as a function of a single variable, the length of the largest bond. Kramers formula [Eq. (2)] is then used to compute the rate of rupture. According to Ref. [3], for a chain of 100 atoms and  $S=0.035$ , this frequency is  $\nu_k=0.273$ , in units of  $\tau_0^{-1}$ . When corrected for the fact that there are  $N$  bonds attempting to break, the rate becomes  $\nu=27.3$  which is about 200 times larger than what is obtained in the simulation.